PROCEEDINGS OF SCIENCE

The all-particle cosmic ray energy spectrum measured with HAWC in the TeV region

J. A. Morales-Soto[a,*] **and J. C. Arteaga-Velázquez**[a] **for the HAWC collaboration**

[a] *Instituto de Física y Matemáticas, Universidad Michoacana, Morelia, Michoacán, México.*

E-mail: jorge.morales@umich.mx, juan.arteaga@umich.mx

The HAWC observatory is an air shower detector well suited for the research of cosmic rays in the energy interval between 10 TeV to 1 PeV, which is very interesting because in this range the data from space-borne detectors and extensive air shower experiments overlap. This fact opens the possibility to perform cross checks between direct and indirect cosmic ray detector techniques and to study the systematic errors that affect each detection technique. In this work, we present an update of the all-particle energy spectrum of cosmic rays between 10 TeV and 1 PeV that was obtained from an unfolding analysis applied on three years of HAWC data. The events were collected from January, 2018 to December, 2020. The results show the presence of a knee-like structure around tens of TeV, which was previously reported by the HAWC collaboration in 2017. For the calibration and the energy estimation, we employed the high-energy hadronic interaction model QGSJET-II-04.

**** 27th European Cosmic Ray Symposium - ECRS ****
**** 25-29 July 2022 ****
**** Nijmegen, the Netherlands ****

*Speaker

PoS(ECRS)087

1. Introduction

The study of cosmic rays dates more than 100 years ago, yet there are many unsolved mysteries around this radiation, related with their sources, acceleration mechanism and propagation in space. Some clues to answer these questions can be found in the study of the energy distribution of these energetic particles. Depending of the energy, the spectrum of cosmic rays can be measured by direct or indirect techniques. In the past, due to technological limitations, direct measurements were mainly constrained to energies below some TeV and indirect techniques, mostly to energies above a few PeV, producing a gap between both detection methods in the TeV energy range.

Recent technological advances, however, have allowed to reduce such a gap. In this regard, the NUCLEON [1], DAMPE [2] and CALET [3] satellites, as well as the HAWC high-altitude air-shower observatory [5] have contributed to this effort.

The HAWC observatory is a ground-based detector for gamma and cosmic rays, located in Puebla, Mexico, between the Pico de Orizaba and the Sierra Negra volcanoes. The detector consists of 300 water Cherenkov detectors and 1200 photomultipliers. Since the development of the experiment, the HAWC collaboration has dedicated its effort to unravel novel insights about gamma rays [4] and cosmic rays [5–7]. One of the most important contributions of the collaboration to the cosmic ray science is the measurement of the total energy spectrum in the energy interval between 10 TeV and 500 TeV, where a new kink on the spectrum was found [5]. The present work is an update of this analysis. For this study, we have increased the size of the data sample, and extended the energy of the spectrum up to 1 PeV. Finally, we have reduced the systematic errors in the reconstruction of the spectrum.

2. HAWC's simulated and experimental data

The simulations employed for the cosmic-ray analysis in HAWC were performed within the framework CORSIKA (v760) [8]. We simulated eight primary nuclei (H, He, C, O, Ne, Mg, Si, and Fe), with a differential energy spectrum of E^{-2} using FLUKA [9] and QGSJET-II-02 [10]. Simulated events possess arrival directions that can go from 0° up to 65°. In order to recreate realistic spectra we weighted the simulations with a composition model based on fits to experimental data from CREAM-II [12], ATIC-02 [13], and PAMELA [14]. Finally, we use GEANT-4 [11] to simulate the detector response of HAWC.

The data used in this analysis were collected in period from January 1st, 2017 to December 31st, 2020. The effective time of observation amounts to 2.9 years.

The primary energy of the cosmic-ray events in HAWC is determine through a log-likelihood analysis in which the lateral distribution is compared event-by-event and the result is stored in probability tables divided per bins of energy, and zenith angle.

For further details about the primary energy reconstruction method in HAWC and other air-shower reconstruction procedures see [5, 6].

3. Selecting the data

To reconstruct the energy spectrum we must apply cuts to rule out events that can potentially increase the systematic effects in our result that are mostly associated to errors in the reconstruction

of main shower observables such as the primary energy, arrival direction, and core position. It is important to mention that the event selection was chosen after studies with our MC simulations. As a first selection criterion we considered only those events that were successfully reconstructed (according to the method described in [4]). Next, we restricted the selection to showers with zenith angles within 0° and 35°, and whose reconstructed shower cores were located mainly inside HAWC's area. Additionally, we required that events activated a minimum of 60 photomultipliers within a radius of 40 m from the core of the event, and that have hits in at least 30% of the active photomultipliers (PMT). Finally, for the selection, we restricted the data to the reconstructed energy interval $\log_{10}(E^r/GeV) = [3.8, 6.2]$.

4. Reconstruction of the total energy spectrum

We begin the analysis by reconstructing the raw energy distribution, $N(E^r)$, from the measured data described in section 2, with a bin size of $\Delta \log_{10}(E^r/\mathrm{GeV}) = 0.2$. As expected, this raw distribution (see Fig. 1) needs to be corrected for migration effects, and to do so we made use of an unfolding procedure based on the Bayes theorem [15–17].

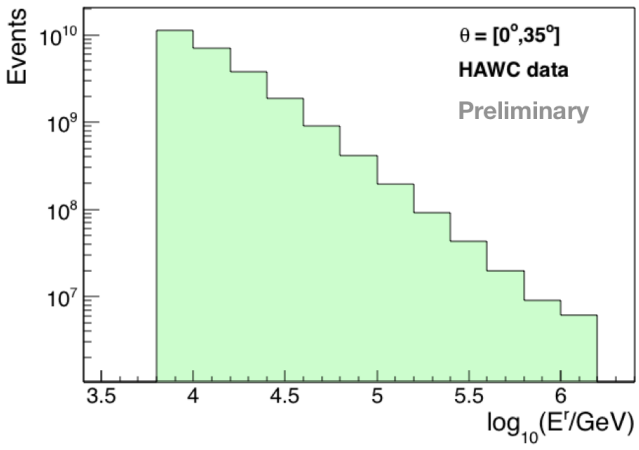

Figure 1: Raw energy distribution, $N(E^r)$, of the selected HAWC data used in the present analysis (see section 2).

For the unfolding procedure, we employed the MC simulations with our cosmic-ray composition model to build the response matrix (see Fig. 2, left), $P(E^r|E)$. With these simulations, we also computed the effective area (Fig. 2, right) using the formula

$$A_{\mathrm{eff}}(E) = A_{\mathrm{thrown}} \cdot \epsilon(E). \tag{1}$$

where $\epsilon(E)$ is the efficiency for detecting a shower event with energy E, and A_{thrown} stands for the simulated throwing area. Such area corresponds to a circular region over where the simulated events were thrown ($R_{\mathrm{thrown}} = 1$ km), and it is multiplied by a geometrical factor due to the flat geometry of the array. In other words, the effective area is the region in which an event will be detected, reconstructed and pass the cuts described in section 3. A detailed description can be found in [5].

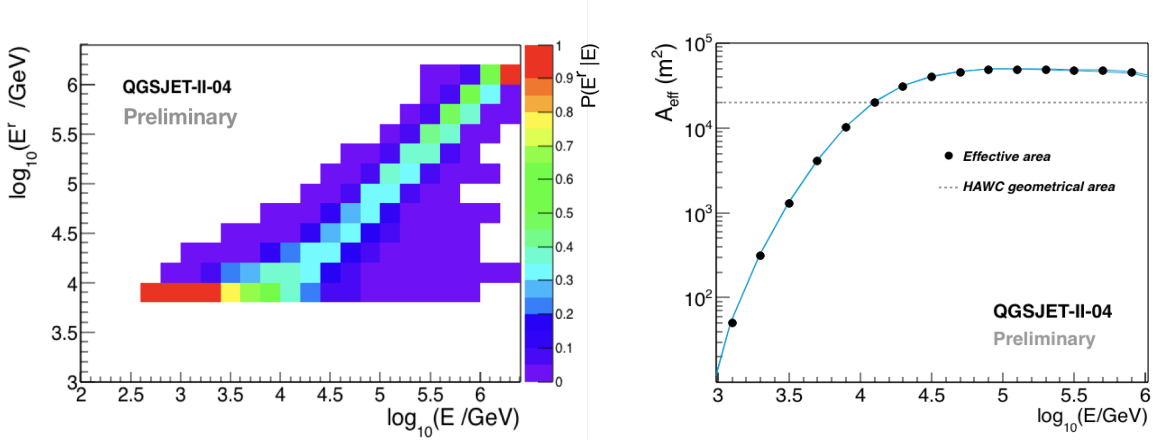

Figure 2: *Left*: Response matrix, $P(E^r|E)$, used in our analysis. *Right*: Effective area for the reconstruction of the energy spectrum of cosmic rays as a function of the true primary energy E, compared with the geometric area of HAWC (dashed line). Both, response matrix and effective area, were calculated with our MC simulations, using the hadronic interaction model QGSJET-II-04 (see section 2).

Once all these elements are computed, we estimated the energy spectrum by means of the following expression:

$$\Phi(E) = \frac{N(E)}{\Delta E \; T \; \Delta\Omega \; A_{\text{eff}}}, \tag{2}$$

where $N(E)$ is the unfolded spectrum, ΔE represents the energy bin width ($\Delta \log_{10}(E/\text{GeV}) = 0.2$), T is the total effective time and equals to 1062 days, $\Delta\Omega$ corresponds to the solid angle that was monitored with a value of 1.14 sr, and A_{eff} is the effective area (described above).

5. Results

The left plot in Fig. 3 shows the unfolded energy spectrum obtained from this analysis. The systematic errors are shown with an error band, while the statistical uncertainties are represented with vertical error bars. The systematic error sources that were included in our analysis are uncertainties in the effective area, the composition model of cosmic rays, differences between experimental runs (divided in periods of one month), the quantum efficiency, resolution and charge resolution of the PMTs, and the late light effect [4]. Also, we included uncertainties due to the unfolding technique by reconstructing the energy spectrum with a different unfolding algorithm (Gold's technique [18]) and by accounting the differences between the resulting spectrum and our main result as uncertainties, and by studying also the dependence with the prior and the smoothing algorithm.

In our result, we found a cut in the energy spectrum of cosmic rays in the TeV energy region, thus we performed a statistical analysis to find out the significance of this feature. To start the aforementioned analysis, we used a χ^2 minimization procedure (following the definition from [19]) to fit our main result with a single power-law function

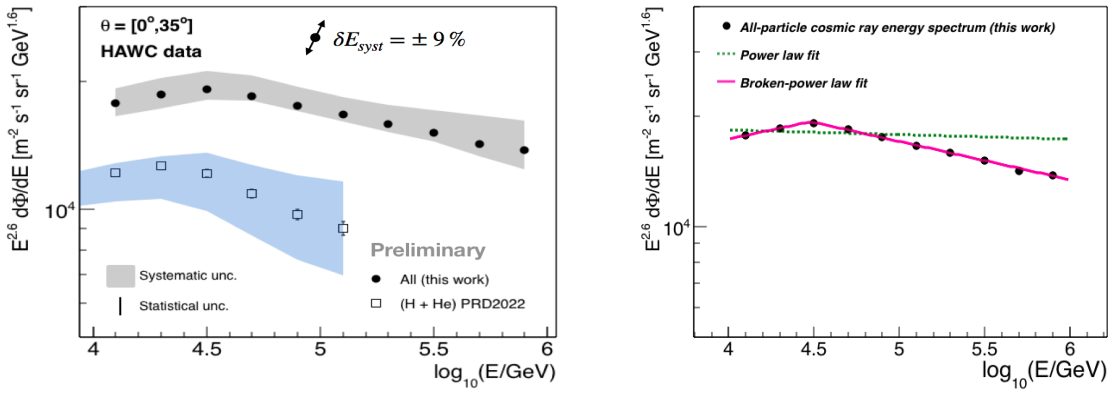

Figure 3: *Left: The all-particle cosmic ray energy spectrum measured with HAWC (black circles). In here, it is compared with the spectrum of the H+He mass group of cosmic rays from [6] (open squares). Spectra are shown with their corresponding systematic uncertainties (error bands) and statistical errors (vertical error bars). Right: Results of the fits to the HAWC spectrum with a power-law formula (green dashed line) and a broken power-law expression (pink continuous line).*

$$\Phi(E) = \Phi_0 E^{\gamma_1}. \tag{3}$$

In equation (3), Φ_0 is simply a normalization parameter, and γ_1 is the spectral index. The corresponding parameter values from the fit are $\Phi_0 = 10^{4.47\pm0.01}$ m^{-2} s^{-1} sr^{-1} GeV^{-1} and $\gamma_1 = -2.650 \pm 0.001$ with $\chi^2_0 = 418.84$ for a total of 8 degrees of freedom. Now, we proceed to fit our main result again, but this time with a broken power-law function

$$\Phi(E) = \Phi_0 E^{\gamma_1} \left[1 + \left(\frac{E}{E_0}\right)^{\epsilon}\right]^{(\gamma_2-\gamma_1)/\epsilon}, \tag{4}$$

which gives us $\Phi_0 = 10^{3.80\pm0.04}$ m^{-2} s^{-1} sr^{-1} GeV^{-1}, $\gamma_1 = -2.5 \pm 0.01$, $\gamma_2 = -2.7 \pm 0.01$, $\epsilon = 9.9 \pm 1.8$, and $E_0 = (31.02^{+1.92}_{-1.81})$ TeV with $\chi^2_1 = 0.17$ for 5 degrees of freedom. The χ^2 value is small due to the size of the statistical error of the unfolded energy spectrum. This effect comes from the iteration depth in the unfolding procedure. The corresponding error increases with the iteration depth. The right plot in Fig. 3 shows both fits over the energy spectrum.

Once we have the information from the fits, we want to find which hypothesis best describes the data, thus we employed a statistical analysis based on a test statistic that is defined as $TS = \Delta\chi^2 = \chi^2_0 - \chi^2_1$. For the observed spectrum, we found $TS_{obs} = 406.15$. Then, we generate toy MC spectra with correlated data points using our statistical covariance matrix and the results of the fit for the power-law model [19], and for each MC spectrum, we repeated the fits with eqs. (3) and (4). The results gives us a distribution of TS for the hypothesis of the power-law scenario and from it we found a *p-value* $p \leq 4 \times 10^{-5}$, giving the broken power-law scenario a significance of at least 3.9σ.

Finally, in Fig. 4 we compared the unfolded energy spectrum with measurements from other cosmic ray experiments (space-borne and ground-based detectors). The measurements come from the satellites ATIC-02 [20] and NUCLEON [1], and from the indirect cosmic ray experiments

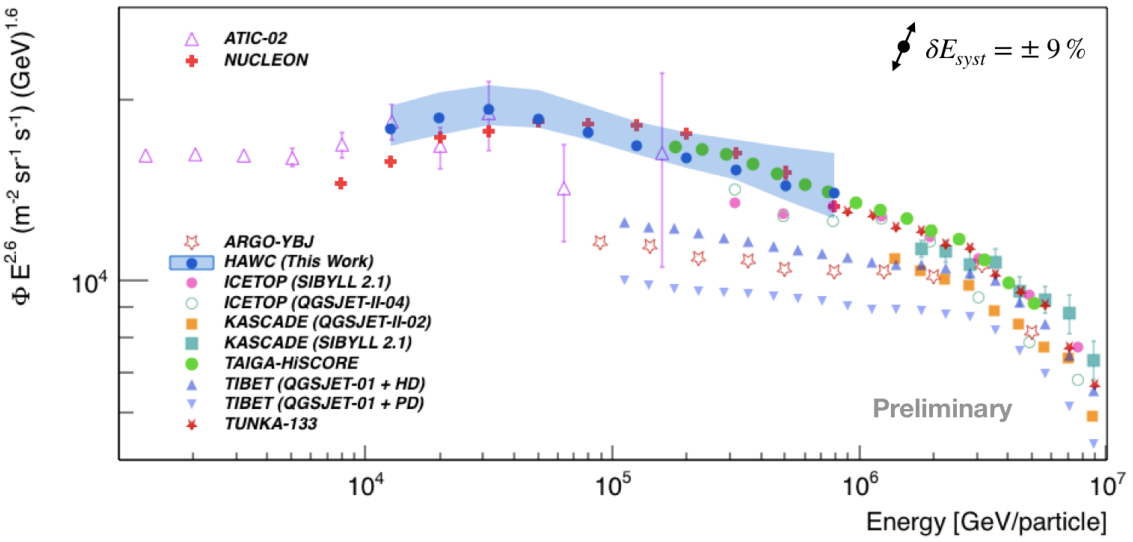

Figure 4: Comparison of the HAWC all-particle energy spectrum of cosmic rays (black circles, this work) and other measurements of the spectrum from direct and indirect cosmic-ray experiments (refer to end of section 5).

ARGO-YBJ [21], ICETOP [22], KASCADE [23, 24], TAIGA-HiSCORE [25], TIBET [26] and TUNKA-133 [27].

6. Discussion

We have reduced the systematic uncertainties of the HAWC energy spectrum in comparison with the analysis of [5] thanks to the recent improvements in the PMT modeling [4]. Just as a reference value for the aforesaid comparison, at energies of E = 100 TeV, the systematic uncertainty was reduced from -24.8%/+26.4% to -3.7%/+9.8%.

Another important point to be discuss here is the shape of the energy spectrum in the energy range from 10 TeV to 1 PeV. According to the present analysis, the total energy spectrum of cosmic rays is best described by a broken power-law. The presence of a spectral difference on the spectrum in the TeV region is also supported by NUCLEON data [1].

Finally, Fig. 4 shows an agreement of our result with ATIC-02 data [20] at energies close to 10 TeV and with TAIGA-HiSCORE [25] at around 1 PeV. The HAWC result, however, is larger than ARGO-YBJ, TIBET and ICETOP measurements at high energies.

7. Conclusions

In this work, we have improved the analysis on the total energy spectrum of cosmic rays with HAWC data, thus contributing to the now increasing overlap between direct and indirect cosmic-ray measurements in the 10 TeV - 1 PeV energy regime. In this region, our result is found to be in agreement (within systematic uncertainties) with the observations made by NUCLEON [1]. Both

NUCLEON and HAWC show a softening in the energy spectrum at TeV energies. In particular, HAWC measurements show a softening around an energy of 31 TeV.

Acknowledgements

We acknowledge the support from: the US National Science Foundation (NSF); the US Department of Energy Office of High-Energy Physics; the Laboratory Directed Research and Development (LDRD) program of Los Alamos National Laboratory; Consejo Nacional de Ciencia y Tecnología (CONACyT), México, grants 271051, 232656, 260378, 179588, 254964, 258865, 243290, 132197, A1-S-46288, A1-S-22784, cátedras 873, 1563, 341, 323, Red HAWC, México; DGAPA-UNAM grants IG101320, IN111716-3, IN111419, IA102019, IN110621, IN110521; VIEP-BUAP; PIFI 2012, 2013, PROFOCIE 2014, 2015; the University of Wisconsin Alumni Research Foundation; the Institute of Geophysics, Planetary Physics, and Signatures at Los Alamos National Laboratory; Polish Science Centre grant, DEC-2017/27/B/ST9/02272; Coordinación de la Investigación Científica de la Universidad Michoacana; Royal Society - Newton Advanced Fellowship 180385; Generalitat Valenciana, grant CIDEGENT/2018/034; Chulalongkorn University's CUniverse (CUAASC) grant; Coordinación General Académica e Innovación (CGAI-UdeG), PRODEP-SEP UDG-CA-499; Institute of Cosmic Ray Research (ICRR), University of Tokyo, H.F. acknowledges support by NASA under award number 80GSFC21M0002. We also acknowledge the significant contributions over many years of Stefan Westerhoff, Gaurang Yodh and Arnulfo Zepeda Dominguez, all deceased members of the HAWC collaboration. Thanks to Scott Delay, Luciano Díaz and Eduardo Murrieta for technical support.

In addition, J.A.M.S. and J.C.A.V. also want to thank the partial support from CONACYT grant A1-S-46288, and the Coordinación de la Investigación Científica de la Universidad Michoacana.

References

[1] V. Grebenyuk, and the NUCLEON collaboration. Advances in Space Research, 64(12), 2546-2558 (2019).
[2] Q. An, R. Asfandiyarov, and the DAMPE collaboration. Science Advances, 5(9), 3793 (2019).
[3] O. Adriani, Y. Akaike, and CALET Collaboration. Physical Review Letters, 122 (18), 181102 (2019).
[4] A. U. Abeysekara, and the HAWC Collaboration. The Astrophysical Journal, 881(2), 134 (2019).
[5] R. Alfaro, and the HAWC Collaboration. Physical Review D, 96(12), 122001 (2017).
[6] J. C. Arteaga-Velázquez, and the HAWC collaboration Physical Review D, 105(6), 063021 (2022).
[7] A. U. Abeysekara, and the HAWC collaboration. ApJ, 865, 57 (2018).
[8] D. Heck, J. Knapp, J. N. Capdevielle, et al. Report FZKA 6019. Forschungszentrum Karlsruhe (1998).
[9] G. Battistoni, F. Cerutti, A. Fasso, et al. In AIP Conference proceedings Vol. 896, No. 1, pp. 31-49 (2007).
[10] S. Ostapchenko. Physical Review D, 83(1), 014018 (2011).
[11] S. Agostinelli, and the Geant4 Collaboration. Nuclear instruments and methods in physics research section A, 506(3), 250-303 (2003).
[12] H. S. Ahn et al. (CREAM Collaboration), Astrophys. J. 707, 593 (2009).
[13] M. Aguilar et al. (AMS Collaboration), Phys. Rev. Lett. 115, 211101 (2015).
[14] O. Adriani et al. (PAMELA Collaboration), Science 332, 69 (2011).
[15] G. D'Agostini. Nuclear Instruments and Methods in Physics Research Section A: Accelerators, Spectrometers, Detectors and Associated Equipment 362.2-3 (1995): 487-498.
[16] W. H. Richardson (1972). JoSA, 62(1), 55-59.
[17] L. B. Lucy (1974). The astronomical journal, 79, 745.
[18] R. Gold. Report ANL-6984 (Argonne National Laboratory, USA, 1964).

[19] R. Workman, and the Particle Data Group, Review of particle physics To be published (2022).
[20] A. D. Panov, J. H. Adams, et al. (2009). Bulletin of the Russian Academy of Sciences: Physics, 73(5), 564-567.
[21] P. Montini, et al. ArXiv, preprint arXiv:1608.01389, 2016.
[22] M. G. Aartsen, and the ICECUBE collaboration, Physical Review D, 102 (2020).
[23] W. Apel, J. Arteaga-Velázquez, et al., Astroparticle Physics, vol. 47, pp. 54–66, 2013.
[24] T. Antoni, W. Apel, et al., Astroparticle physics, vol. 24, no. 1-2, pp. 1–25, 2005
[25] V. Prosin, I. Astapov, et al. (2019). Bulletin of the Russian Academy of Sciences: Physics, 83(8), 1016-1019.
[26] M. Amenomori, X. Bi, et al., The Astrophysical Journal, vol. 678, no. 2,p. 1165, 2008.
[27] V. Prosin, et al., NuclearInstruments and Methods in Physics Research Section A, vol. 756, pp. 94–101, 2014.